

# Metastable transitions in inertial Langevin systems: what can be different from the overdamped case?

Andre N. Souza<sup>a</sup>, Molei Tao<sup>a</sup>

<sup>a</sup>*School of Mathematics, Georgia Institute of Technology, Atlanta, GA 30332 USA*

---

## Abstract

Although the overdamped limit of the Langevin equation is a reversible diffusion process governed by a gradient system, the inertial Langevin system is irreversible, non-gradient, and non-uniformly-elliptic. Consequently, metastable transitions in Langevin dynamics can exhibit rich behaviors that are markedly different from the overdamped limit. For instance, when the dissipation is weak, heteroclinic connections that exist in the overdamped limit do not necessarily have a counterpart in the Langevin system, potentially leading to different transition rates. Furthermore, when the friction coefficient depends on the velocity, the overdamped limit no longer exists, but it is still possible to efficiently find instantons. The approach we employed for these discoveries was based on (i) a rewriting of the Freidlin-Wentzell action in terms of time-reversed dynamics, and (ii) an adaptation of the string method, which was originally designed for gradient systems, to this specific non-gradient system.

*Keywords:* Freidlin-Wentzell action, instanton, inertial Langevin equation, underdamped dynamics, matrix-valued variable friction coefficient.

---

## 1. Introduction

The Langevin equation

$$\begin{aligned} dX &= V dt \\ M dV &= -\Gamma V dt + f(X) dt + \epsilon \Gamma^{1/2} dW \end{aligned} \tag{1}$$

can exhibit richer behaviors than its overdamped limit

$$dX = \Gamma^{-1} f(X) dt + \epsilon \Gamma^{-1/2} dW, \tag{2}$$

where  $M \in \mathbb{R}^{n \times n}$  is a positive definite mass matrix,  $\Gamma \in \mathbb{R}^{n \times n}$  is a positive definite friction coefficient matrix, the variables  $X, V \in \mathbb{R}^n$ ,  $\epsilon \in \mathbb{R}$ , and  $W$  is an  $n$ -dimensional Wiener process. When  $\epsilon = 0$  the equations are deterministic and play a special role in the  $\epsilon \rightarrow 0$

---

*Email addresses:* `andre.souza@gatech.edu` (Andre N. Souza), `mtao@gatech.edu` (Molei Tao)

limit. We also refer to the  $\epsilon = 0$  case by the same names, but when ambiguity arises we will add the term “noiseless” to distinguish the two cases.

Let  $\|\cdot\|_A$  denote a weighted norm,

$$\|\mathbf{x}\|_A = \sqrt{\mathbf{x}^T A \mathbf{x}}, \quad (3)$$

where  $\mathbf{x} \in \mathbb{R}^n$  and  $A \in \mathbb{R}^{n \times n}$  is a positive definite matrix. Freidlin-Wentzell theory shows the transition from one point in the state space to another of 1 or 2 is characterized by the minimizer of the following actions

$$L[\mathbf{x}] = \int_0^T \|M\ddot{\mathbf{x}} + \Gamma\dot{\mathbf{x}} - \mathbf{f}\|_{\Gamma^{-1}}^2 dt \quad (4)$$

and

$$O[\mathbf{x}] = \int_0^T \|\dot{\mathbf{x}} - \Gamma^{-1}\mathbf{f}\|_{\Gamma}^2 dt \quad (5)$$

in the limit  $\epsilon \rightarrow 0$ , respectively (see e.g., [1, 2]).

The minimizers of these functionals are often called instantons. They give a higher order correction to the leading order approximation of noiseless dynamics, taking into account the long-term effects of small noise.

Of particular interest is when  $\mathbf{f}$  is the gradient of a potential, i.e.  $\mathbf{f} = -\nabla U$  for a function  $U : \mathbb{R}^n \rightarrow \mathbb{R}$ . Suppose one is interested in the transition from a local minimum  $\mathbf{x}_A$  of  $U$  to a saddle point  $\mathbf{x}_S$ . If there exists a heteroclinic connection from  $\mathbf{x}_S$  to  $\mathbf{x}_A$  in the noiseless overdamped system as well as a heteroclinic connection in a modification of the noiseless Langevin system, then the values of the functionals 4 and 5 coincide; see §2. However, the existence of a heteroclinic connection in the former system does not guarantee the existence for a counterpart in the latter. As we will see in §4.2, if the friction coefficient is sufficiently low, the correspondence between these two heteroclinic connections can be broken. More generally, if the friction coefficient matrix has at least one sufficiently low eigenvalue, this possibility exists.

Consequently, the minimizing paths themselves can also be markedly different between the overdamped limit and the Langevin equation. We will describe how to compute the Langevin instantons in §3, based on structures of the functionals 4 and 5 illustrated in §2. It is oftentimes possible to leverage computations from the overdamped equation to obtain instantons for the Langevin functional, and the string method [3, 4] originally designed for overdamped Langevin only needs to undergo a slight change to adapt to a matrix-valued friction coefficient that depends on position and velocity. However, for reasons just mentioned, it is still possible to miss local minimizers of the action 4, and when this happens, we resort to the first-order optimality condition of Euler-Lagrange equation, which is only utilized in §4.2 for understanding the differences between underdamped and overdamped Langevin equations.

§4 discusses the details of the Langevin transition problem in cases, with increasing complexity based on different kinds of positive definite friction coefficient matrices:

1. **Constant Overdamped.** When the eigenvalues of the friction coefficient are large, the overdamped limit and the Langevin equation bare many similarities. This case is well-known and well studied (see for instance, [5], [6], [7], [8]). §4.1 provides a concise review.
2. **Constant Underdamped.** When the eigenvalues of the friction coefficient matrix are sufficiently low, new phenomena distinctive from the overdamped limit can arise in the Langevin system. Physically this case may be motivated by considering situations where inertial effects are important. Difference appears when heteroclinic connections in the overdamped limit have no analog in the corresponding Langevin equation. Additionally, it is no longer the case that the global minimizer of the Freidlin-Wentzell action is a “time-reversed” trajectory. We first illustrate this using a standard 4-dimensional test problem and then provide an explanation based on semi-analytical understanding of a 2-dimensional example in §4.2. Note that there have been great work on friction approaching zero asymptotics (e.g., [8, 9]), and the scope of this article is complementary as we focus on finite friction coefficients and masses.
3. **Position Dependent.** Our formulation allows for the consideration of non-constant friction coefficient matrices. This part focuses on position dependent ones. See [10] and references therein for why such frictions are worth studying. Another motivation for position-dependent friction is to model certain biological systems – when interactions with a solvent are modeled by noise and friction, the hydrophobic and hydrophilic regions of lipid bilayer, for instance, correspond to different friction coefficients [11]. To illustrate what difference can be induced by the position dependence, we give an example in §4.3, where we see that a localized change in the friction coefficient at a critical location can lead to a global change in the instanton. Two different definitions of an overdamped ‘limit’ will also be discussed — one preserves the invariant distribution of Boltzmann-Gibbs, and the other is consistent in terms of rare events.
4. **Velocity Dependent:** Our formulation also allows for the consideration of (both position and) velocity dependent friction coefficients, even though there is no more overdamped limit and Boltzmann-Gibbs is in general no longer an invariant distribution either. Velocity dependent friction coefficient can be viewed as a more flexible model of friction allowing for deviations from linear models [12, 13]. The long term goal is to be able to address more complicated frictions such as those used to model swarming (e.g., [14, 15]) and astrophysical dissipation (e.g., [16, 17]), but investigations in this article are restricted to cases when zero velocity corresponds to stable fixed points or saddles.  
To correctly compute instantons in the presence of velocity dependent friction coefficient (i.e., friction nonlinear in velocity), modifications need to be made. In particular, if the friction is not symmetric with respect to sign change in velocity, one has to consider **two** Langevin-type systems. See §4.4.

There are many great surveys of how to find minimizing trajectories in dynamical systems with noise, and here we provide an incomplete list of two most recent ones, [18] and [19]. The Langevin system considered here may be understood formally via a transverse

decomposition of a first-order system (see [20] and additionally [21]), however the noise is degenerate (i.e., non-uniformly-elliptic diffusion). Versatile numerical methods based on action minimization such as [22, 23, 24, 25, 26, 27, 28, 29, 18] work for nongradient systems and infinite dimensional systems too, but their applications to our system require adaptations, also due to the degenerate noise. Powerful theories based on hypoellipticity [30, 31] and hypocoercivity [32] do provide tools for analyzing the degenerate and irreversible (but not too irreversible) system of Langevin, but our simple theory will not require them.

## 2. Problem Formulation

In order to simplify analysis of the Langevin equation, we first change to mass coordinates, as in [33],  $X = M^{-1/2}Q$ ,  $V = M^{-1/2}W$ ,  $U(X) = Z(Q)$ ,  $\frac{\partial Q}{\partial X} = M^{1/2}$ , so that

$$\begin{aligned} dX &= V dt \\ M dV &= -\Gamma V dt - \partial_X U dt + \epsilon \Gamma^{1/2} dW \end{aligned} \quad (6)$$

becomes

$$\begin{aligned} dQ &= W dt \\ dW &= -M^{-1/2} \Gamma M^{-1/2} W dt - \partial_Q Z dt + \epsilon M^{-1/2} \Gamma^{1/2} dW. \end{aligned} \quad (7)$$

The correlation matrix is  $M^{-1/2} \Gamma^{1/2} (M^{-1/2} \Gamma^{1/2})^T = M^{-1/2} \Gamma M^{-1/2}$ , thus we may effectively replace the this system by

$$\begin{aligned} dQ &= W dt \\ dW &= -M^{-1/2} \Gamma M^{-1/2} W dt - \partial_Q Z dt + \epsilon (M^{-1/2} \Gamma M^{-1/2})^{1/2} dW \end{aligned} \quad (8)$$

without changing relevant statistics. In these coordinates we have a system of identity mass with effective friction coefficient  $M^{-1/2} \Gamma M^{-1/2}$ . In this regard low mass and high friction are similar. Thus, with this rescaling in mind, we take mass to be the identity matrix from now on.

Although the global minimizers are the only one relevant for the most likely transitions, we relax this requirement and content ourselves with computing local minimizers. The rationale is that local minimizers are often associated to dynamical structures such as saddle points (see (9) and (10) and discussions that follow), and if one can exhaust these structures (this is often easier), all local minimizers and hence the global one, can be found. We are interested in the case where the position boundary conditions coincide for both functionals,  $\mathbf{x}(0) = \mathbf{x}_A$ ,  $\mathbf{x}(T) = \mathbf{x}_B$ , and the Langevin function is augmented with additional velocity boundary conditions,  $\dot{\mathbf{x}}(0) = \mathbf{v}_A$ ,  $\dot{\mathbf{x}}(T) = \mathbf{v}_B$ . We typically choose homogeneous velocity boundary conditions,  $\mathbf{v}_A = \mathbf{v}_B = \mathbf{0}$ .

Utilizing the identity  $\|a + b\|^2 = \|a - b\|^2 + 4\langle a, b \rangle$  we rewrite the functionals 4 and 5 as

follows,

$$\begin{aligned}
L_T[\mathbf{x}] &= \int_0^T \|\ddot{\mathbf{x}} + \Gamma \dot{\mathbf{x}} + \nabla U\|_{\Gamma^{-1}}^2 dt \\
&= \int_0^T \|\ddot{\mathbf{x}} - \Gamma \dot{\mathbf{x}} + \nabla U\|_{\Gamma^{-1}}^2 dt + 4 \dot{\mathbf{x}}^T (\ddot{\mathbf{x}} + \nabla U) dt \\
&= \int_0^T \|\ddot{\mathbf{x}} - \Gamma \dot{\mathbf{x}} + \nabla U\|_{\Gamma^{-1}}^2 dt + 4 \left[ \frac{1}{2} \|\mathbf{v}_B\|^2 - \frac{1}{2} \|\mathbf{v}_A\|^2 + U(\mathbf{x}_B) - U(\mathbf{x}_A) \right]
\end{aligned} \quad (9)$$

and

$$\begin{aligned}
O_T[\mathbf{x}] &= \int_0^T \|\dot{\mathbf{x}} + \Gamma^{-1} \nabla U\|_{\Gamma}^2 dt \\
&= \int_0^T \|\dot{\mathbf{x}} - \Gamma^{-1} \nabla U\|_{\Gamma}^2 + 4 \dot{\mathbf{x}}^T \nabla U dt \\
&= \int_0^T \|\dot{\mathbf{x}} - \Gamma^{-1} \nabla U\|_{\Gamma}^2 dt + 4 [U(\mathbf{x}_B) - U(\mathbf{x}_A)].
\end{aligned} \quad (10)$$

These calculations show that the functionals are bounded below, i.e.

$$L_T[\mathbf{x}] \geq \max \left\{ 4 \left[ \frac{1}{2} \|\mathbf{v}_B\|^2 - \frac{1}{2} \|\mathbf{v}_A\|^2 + U(\mathbf{x}_B) - U(\mathbf{x}_A) \right], 0 \right\} \quad (11)$$

$$O_T[\mathbf{x}] \geq \max \{ 4 [U(\mathbf{x}_B) - U(\mathbf{x}_A)], 0 \} \quad (12)$$

and in particular the lower bounds coincide if  $\|\mathbf{v}_B\|^2 - \|\mathbf{v}_A\|^2 = 0$ .

The two main cases that we focus on here are

- The transition from a saddle point  $\mathbf{x}_S$  to a local minimum  $\mathbf{x}_B$  of  $U$ , with velocity boundary conditions  $\mathbf{v}_A = \mathbf{v}_B = 0$ , abbreviated  $\mathbf{x}_S \rightarrow \mathbf{x}_B$ .
- The transition from a local minimum  $\mathbf{x}_A$  to a saddle point  $\mathbf{x}_S$  of  $U$ , with velocity boundary conditions  $\mathbf{v}_A = \mathbf{v}_B = 0$ , abbreviated  $\mathbf{x}_A \rightarrow \mathbf{x}_S$ .

The velocity and position boundary conditions guarantee that we are considering transitions between fixed points in both the Langevin and overdamped case. From this point on we consider the  $T \rightarrow \infty$  limit.

In the former case, if there exists a heteroclinic connection in the deterministic dynamics (for both systems) from  $\mathbf{x}_S$  to  $\mathbf{x}_B$  then the minimum action is 0, since the minimizer is exactly given by deterministic dynamics (in the infinite time limit), i.e.

$$\ddot{\mathbf{x}} + \Gamma \dot{\mathbf{x}} + \nabla U = 0 \quad (13)$$

$$\dot{\mathbf{x}} + \Gamma^{-1} \nabla U = 0. \quad (14)$$

However, it is possible for heteroclinic connections that exist in 14 to not exist in 13 and vice versa as we show in §4.2.

For  $\mathbf{x}_A \rightarrow \mathbf{x}_S$  it is also possible to find the minimizing trajectory which achieves equality in 11 and 12. We first focus on the case where  $\Gamma$  depends only on position and assume that there exists a heteroclinic connection from  $\mathbf{x}_A$  to  $\mathbf{x}_S$  in the following systems:

$$\ddot{\mathbf{x}} - \Gamma(\mathbf{x})\dot{\mathbf{x}} + \nabla U = 0 \quad (15)$$

$$\dot{\mathbf{x}} - \Gamma^{-1}(\mathbf{x})\nabla U = 0 \quad (16)$$

In this case, these connections are the action minimizing trajectories. Reversing time  $\tau = T - t$ , and denoting derivatives with respect to the new variable with  $'$ , i.e.  $\dot{x} = x'$ , we see

$$\mathbf{x}'' + \Gamma(\mathbf{x})\mathbf{x}' + \nabla U(\mathbf{x}) = 0 \quad (17)$$

$$\mathbf{x}' + \Gamma^{-1}(\mathbf{x})\nabla U(\mathbf{x}) = 0 \quad (18)$$

which are exactly the same as 13 and 14 with respect to the new variables. The minimizing trajectory becomes the same as the noiseless trajectory from  $\mathbf{x}_S \rightarrow \mathbf{x}_A$  after a sign change of the velocity variable in the Langevin case.

If the friction coefficient matrix depends on velocity then the minimizing trajectory must satisfy

$$\mathbf{x}'' + \Gamma(\mathbf{x}, -\mathbf{x}')\mathbf{x}' + \nabla U(\mathbf{x}) = 0 \quad (19)$$

which only coincides with 13 if  $\Gamma(\mathbf{x}, -\mathbf{x}') = \Gamma(\mathbf{x}, \mathbf{x}')$ . We call 19 the time-reversed Langevin equation. Note, however, that heteroclinic connections of 19 and 15 do not necessarily need to be in one-to-one correspondence.

If there is no heteroclinic connection between points of phase space, the time-reversed dynamics do not correspond to minimizers. To understand this case better, we directly use the Euler-Lagrange equation of the variational principle (note: the appearance of  $\ddot{\mathbf{x}}$  normally would require the introduction of a jet bundle instead of the standard tangent bundle, but there is no need to concern this technicality because we work with flat position space  $\mathbb{R}^n$ ):

$$A[\mathbf{x}] = \int_0^T \mathcal{L}(\mathbf{x}, \dot{\mathbf{x}}, \ddot{\mathbf{x}}) dt, \quad (20)$$

$$\frac{\delta A}{\delta \mathbf{x}} = \frac{\partial \mathcal{L}}{\partial \mathbf{x}} - \frac{d}{dt} \frac{\partial \mathcal{L}}{\partial \dot{\mathbf{x}}} + \frac{d^2}{dt^2} \frac{\partial \mathcal{L}}{\partial \ddot{\mathbf{x}}} = 0. \quad (21)$$

If the friction coefficient matrix is isotropic  $\Gamma = \gamma \mathbb{I}$  then simplifications occur for the Langevin functional 4 and the Euler-Lagrange equation becomes

$$\frac{d^4}{dt^4} \mathbf{x} - \frac{d^2}{dt^2} \mathbf{f} - \gamma^2 \frac{d^2}{dt^2} \mathbf{x} - \nabla \mathbf{f} \frac{d^2}{dt^2} \mathbf{x} + (\nabla \mathbf{f})^T \mathbf{f} = 0. \quad (22)$$

We may solve this boundary value problem numerically: §3.3 uses gradient descent, a finite time-horizon approximation, and pseudospectral discretization.

### 3. Numerical Methods

To compute minimizers to the Freidlin-Wentzell action 4, we utilize three different methods: the string method, the numerical integration of dynamics, and directly solving the boundary value problem. We review each method and show how to implement them in the following subsections. Their use in practice is illustrated in §4.

#### 3.1. String method

The string method is both a way of locating saddles between local minima as well as a way to approximate local minimizers of the Freidlin-Wentzell action [3], [4]. To utilize this method one proceeds as follows:

1. First define an initial “string”, i.e, a sequence of points from one local minimum to another, or simply a sequence of points that lie across a separatrix. For example, in many cases one can choose a straight line between one local minimum and another.
2. Evolve each point on the string according to the deterministic dynamics for a single time-step.
3. Calculate the total length of the string and then evenly redistribute the set of points on the string.
4. Repeat 2-3 until convergence.

The string method can also be applied to the Langevin system by writing the equation as a first order system and making a few adaptations as the following. As stated in the previous section, once a saddle is located, the minimizer of the Freidlin-Wentzell action from a local minima to a saddle obeys time-reversed dynamics, i.e.

$$\begin{aligned}\dot{\mathbf{x}} &= \mathbf{v} \\ \dot{\mathbf{v}} &= -\nabla U + \Gamma(\mathbf{x}, \mathbf{v})\mathbf{v}\end{aligned}\tag{23}$$

as long as a heteroclinic connection exists between the saddle and the minima. Reversing time, and making the change of variables  $\mathbf{v} = -\mathbf{w}$ , yields the following system

$$\begin{aligned}\mathbf{x}' &= \mathbf{w} \\ \mathbf{w}' &= -\nabla U - \Gamma(\mathbf{x}, -\mathbf{w})\mathbf{w}\end{aligned}\tag{24}$$

where  $\mathbf{x}' = -\dot{\mathbf{x}}$ . This is the noiseless Langevin equation, but with friction coefficient matrix  $\Gamma(\mathbf{x}, -\mathbf{w})$  as opposed to  $\Gamma(\mathbf{x}, \mathbf{w})$ . If the friction coefficient matrix is an even function of the velocity then one can run the string method without modification to compute the correct positions  $\mathbf{x}$  of the string. Once the string has converged, the velocity terms need to undergo a sign flip in the “uphill” part of the string.

If  $\Gamma(\mathbf{x}, -\mathbf{w}) \neq \Gamma(\mathbf{x}, \mathbf{w})$ , the procedure needs to be modified. The easiest solution is to evolve **two** strings. The first obeys the noiseless Langevin dynamics and the latter obeys 24. We call this system the time-reversed (noiseless) Langevin equation. The correct instanton is then a concatenation of different halves (separated by the saddle point) of these two different strings. Which one of the two halves to take as the correct part depends on whether or not

one is computing the transition of minima  $A$  to minima  $B$  or vice versa. Furthermore, a sign flip on velocity still needs to be performed.

It is important to keep in mind that the string method can only compute a local minimizer of the Freidlin-Wentzell action, and different initialization of the string could give rise to different local minimizers. On a practical level, one can try different string initializations and choose the final string that best minimizes the Freidlin-Wentzell action.

### 3.2. Saddle points and dynamics

The Langevin instantons are generally more costly to compute than the overdamped case as they can be more oscillatory and need better resolution. The proposed method in §3.1 cannot fully alleviate this issue either. To reduce the computational cost, knowledge of the overdamped dynamics (when they exist) can be exploited. Such knowledge includes, in particular, the saddle point and the perturbation directions off of that saddle to the local minima. A sufficiently resolved string produces the minimizing path for the overdamped system, which includes the approximate location of a saddle between two minima as well as the perturbation directions. We mention that if one is purely interested in just the saddle, the computation of the string can be avoided, see for example [34, 35]).

When both heteroclinic connections exist (see §2), we utilize these approximate perturbation directions of the overdamped system to obtain approximate perturbation directions of the Langevin system and run dynamics to compute the instanton.

This algorithm proceeds as follows:

1. Calculate the overdamped string.
2. Locate the saddle(s), and then utilize perturbations away from the saddle (as calculated by the string) to obtain perturbation directions for the inertial Langevin system.
3. Simulate the dynamics of the corresponding noiseless Langevin equations. Concatenate to find the instanton.

One way to locate a saddle point on a string is to evaluate the norm of the force at each point on the string and choose the one with  $|\nabla V(q)|^2 \leq \epsilon$ . If heteroclinic connections exist, it is possible to explicitly calculate the correct perturbation direction off the saddle for the Langevin system based on the overdamped result, see §Appendix A. Another possibility is to compute underresolved Langevin strings (i.e. those in §3.1) for approximating the perturbation directions.

### 3.3. Euler-Lagrange equation

To understand what happens when a heteroclinic connection is lost, we also compute instantons directly by numerically solving the Euler-Lagrange equation. This is based on an iterative minimization of the Freidlin-Wentzell action analogous to existing results. In fact, great methods have been developed to compute local minima of 5 as well as nongradient problems. Among them include the minimum action method [22], adaptive minimum action method [23] and its higher-order version [24], and geometric minimum action method [25, 26, 27]. It is also possible to utilize the Hamiltonian formulation to help, see [25, 18, 28]. Note, though, with regards to the Langevin problem considered here, there is no need to use

these more generic and more costly approaches, unless the  $\mathbf{x}_A \rightarrow \mathbf{x}_S$  or  $\mathbf{x}_S \rightarrow \mathbf{x}_B$  heteroclinic connection does not exist (whether they exist is verifiable by methods in §3.1 and §3.2).

Action minimization methods have a natural extension to the Langevin setting 4. For example, one can use gradient-descent and a finite  $T$  approximation to compute minimizers, similar to what was originally done with the minimum action method [22]. Due to the second derivatives arising in the functional, however, the resulting boundary value problem will be fourth-order. Specifically the Euler-Lagrange equations for the Langevin functional are

$$\frac{\delta L}{\delta \mathbf{x}} = \frac{d^4}{dt^4} \mathbf{x} - \frac{d^2}{dt^2} \mathbf{f} - \gamma^2 \frac{d^2}{dt^2} \mathbf{x} - \nabla \mathbf{f} \frac{d^2}{dt^2} \mathbf{x} + (\nabla \mathbf{f})^T \mathbf{f} = 0 \quad (25)$$

under the assumption that the friction coefficient matrix is isotropic,  $\Gamma = \gamma \mathbb{I}$  and identity mass.

As per usual with gradient-descent, we introduce pseudo-time  $\tau$  and evolve

$$\partial_\tau \mathbf{x} = -\frac{\delta L}{\delta \mathbf{x}} \quad (26)$$

forward in pseudo-time until  $\frac{\delta L}{\delta \mathbf{x}}$  is sufficiently small. When discretizing pseudo-time we treat the linear terms implicitly in order to enforce boundary conditions, as is commonly done when evolving partial differential equations. Explicitly, the following boundary value must be solved at every time step

$$\left( \frac{d^4}{dt^4} - \gamma^2 \frac{d^2}{dt^2} + \frac{1}{\Delta\tau} \right) \mathbf{x}_{n+1} = \frac{d^2}{dt^2} \mathbf{f}_n + \nabla \mathbf{f}_n \frac{d^2}{dt^2} \mathbf{x}_n - (\nabla \mathbf{f}_n)^T \mathbf{f}_n + \frac{1}{\Delta\tau} \mathbf{x}_n \quad (27)$$

where  $\Delta\tau$  is the pseudo-time step size. This is a linear boundary value problem for  $\mathbf{x}_{n+1}$  at every time-step.

Amongst the many methods to discretize time  $t$  we utilize a modern form of spectral integration as in [36]. The main idea behind the method is to rewrite 27 in integral form and represent the solution utilizing Chebyshev polynomials. Although derivative operators are dense with respect to Chebyshev collocation points, integral operators in spectral space are banded. This leads to efficient and numerically robust evaluation of solutions. Products and convolutions are computed utilizing the pseudo-spectral method [37].

It is worth noting that one can also compute minimizers to the action

$$\int_0^T (\lambda \|\dot{\mathbf{x}} - \mathbf{v}\|^2 + \|\dot{\mathbf{v}} + \gamma \mathbf{v} - \mathbf{f}\|^2) dt, \quad (28)$$

where  $\lambda$  is a large parameter. The advantage of utilizing this functional is that one can use the same methods that are applied to systems with non-degenerate noise; however, solving 28 leads to a stiff system of equations, resulting in expensive computations. When heteroclinic connections exist, the action minimizer coincides with that of a non-stiff version,

$$\int_0^T (\|\dot{\mathbf{x}} - \mathbf{v}\|^2 + \|\dot{\mathbf{v}} + \gamma \mathbf{v} - \mathbf{f}\|^2) dt, \quad (29)$$

as  $\|\dot{\mathbf{x}} - \mathbf{v}\|^2$  can be made zero pointwise. However, this relaxation may not work if one of the two heteroclinic connections doesn't exist (although when they both exist there is less need to iteratively minimize the action).

## 4. The Differences

In what follows we examine local minimizers of the Langevin action 4 with matrix-valued and possibly position and velocity dependent friction coefficient  $\Gamma$  to highlight generic differences and similarities with its overdamped limit 5 and isotropic friction coefficients. At the end of each section we give generic recommendations on numerical methods.

### 4.1. Large friction coefficient

The overdamped case has been studied extensively as previously mentioned. We also note that the closely related problem of the small mass limit — which we saw in §2 is related to high friction via a rescaling of coordinates — has been analyzed, see e.g., [38, 10, 39, 40]. To recall the phenomenology concretely, we use an illustration based on the Mueller potential

$$U(x, y) = \sum_{i=1}^4 A_i \exp(a_i(x - x_i)^2 + b_i(x - x_i)(y - y_i) + c_i(y - y_i)^2), \quad (30)$$

where the parameters  $A_i, a_i, b_i, c_i, x_i, y_i$  for  $i = 1, \dots, 4$  are chosen the same as [4]. The minimizer here can be computed via the string method or utilizing dynamics.

Figure 1 shows the trajectories of two local minimizers of the Freidlen-Wentzell action with an isotropic (i.e. scalar) friction coefficient  $\gamma = 50$ . We see that, after projecting to position space in the case of Langevin, there is little difference in the trajectories of the Langevin equations and its overdamped limit, except for a small amount of overshoot in the Langevin dynamics.

In the high friction scenario this agreement is generic. If  $\gamma$  is much larger than the spectral radius of the Hessian of  $U$  in the domain of interest, the friction is high enough to justify the overdamped limit.

*Recommendation.* The general recommendation for this case is to focus on the overdamped limit, and the string method in its original form is a good choice for computing the instanton.

### 4.2. Small constant scalar friction coefficient

As we lower the friction coefficient, new situations may arise since inertial effects can now compete with the potential. We first illustrate this in the Mueller system and then provide a detailed analysis of a system with a sixth-order polynomial potential. The features mentioned here are generic and we have observed similar behavior in other systems.

We apply the method of §3.2 to various dissipation regimes of the Mueller system. When the friction becomes small but not too small,  $\gamma = 6$  for instance in this case, oscillatory behaviors near minima are seen in the instanton (left panel of Figure 2). These oscillations can be intuitively understood as an inertial effect due to the fact that the particle cannot

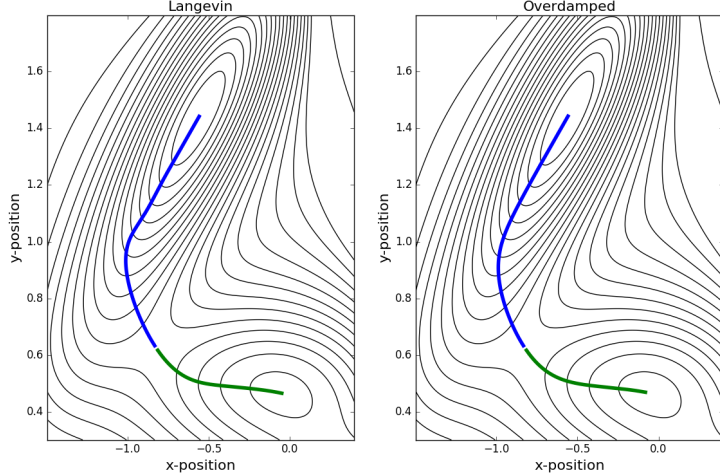


Figure 1: [Color online] Instantons for the Langevin functional (left) and the overdamped functional (right). The primary difference between the two is a slight overshoot in the blue trajectory for the Langevin equation.

stop or take sharp turns instantaneously, unless a lot of noise is used. However, the topology of the transition remains the same as the overdamped instanton so far.

Further lowering the friction coefficient, for instance to  $\gamma = 4$ , leads to a dynamical trajectory that settles to a different minimum, see the right panel of Figure 2. In this case, the particle has enough momentum to overcome intermediary minimum and ends up in another minimum of the potential. One may think that this means a better perturbation direction needs to be chosen for a correct departure from the saddle point; however, there is actually another possibility: there no longer exists a heteroclinic connection between the saddle and the original target minimum.

To understand this possibility of losing heteroclinic connection, let us consider a simpler, one degree-of-freedom example (space is therefore 1D), where the potential is given by a sixth-order polynomial

$$U(x) = \sum_{i=1}^6 a_i x^i. \quad (31)$$

$a_i \in \mathbb{R}$  for  $i = 1, \dots, 6$  are such that there are three local minima at positions  $x_A \leq x_B \leq x_C$  and saddles  $x_{AB} \leq x_{BC}$ . Furthermore  $U(x_{ab}) \geq U(x_{bc}) \geq U(x_b) \geq U(x_a) \geq U(x_c)$ . See Figure 3 for an example.

In the overdamped limit, the state space is 1-dimensional, and the transitions between different minima can only go through one path, i.e. the transition from  $x_A \rightarrow x_C$  has to first pass through the minima at  $x_B$ . Furthermore the transitions must also pass through the saddles at  $x_{AB}$  and  $x_{AC}$ .

In the Langevin system, however, this is not necessarily the case since the state space is 2-dimensional. More precisely, the transition path of  $x_A \rightarrow x_B$  changes with the amount of

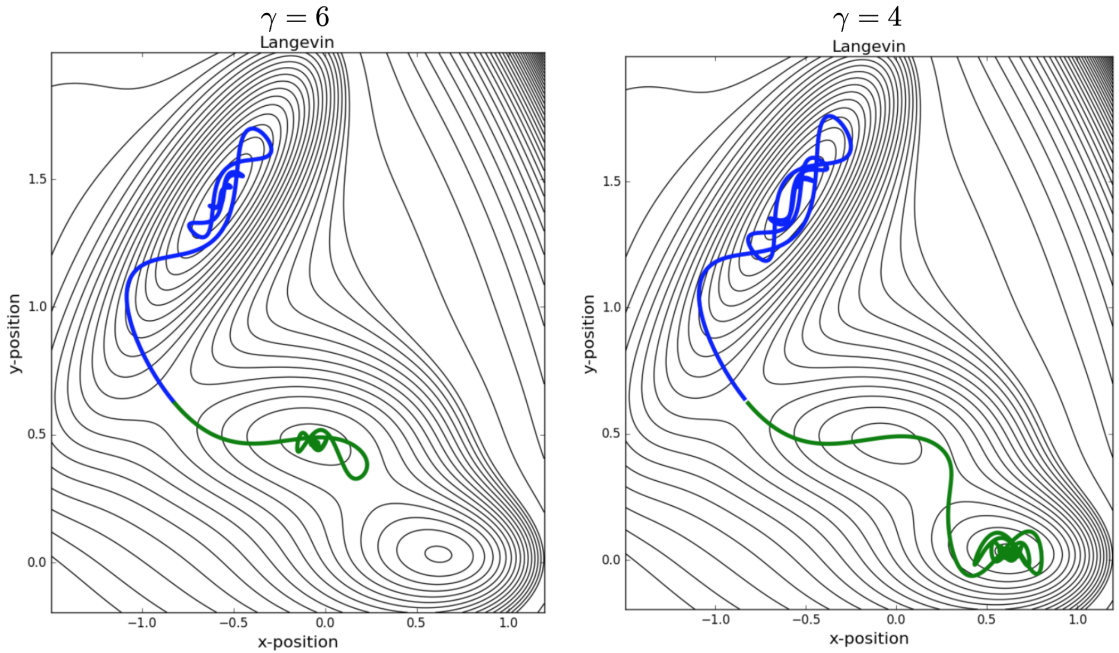


Figure 2: [Color online] Dynamical trajectories of the Langevin equation for different friction coefficients in the underdamped regime. On the left ( $\gamma = 6$ ) the dynamical trajectories settle to the same minima as the overdamped scenario. In this case the trajectory also coincides with the instanton for the system. As we further decrease the friction coefficient to  $\gamma = 4$  the same perturbation direction leads to a dynamical trajectory that settles to a different minimum.

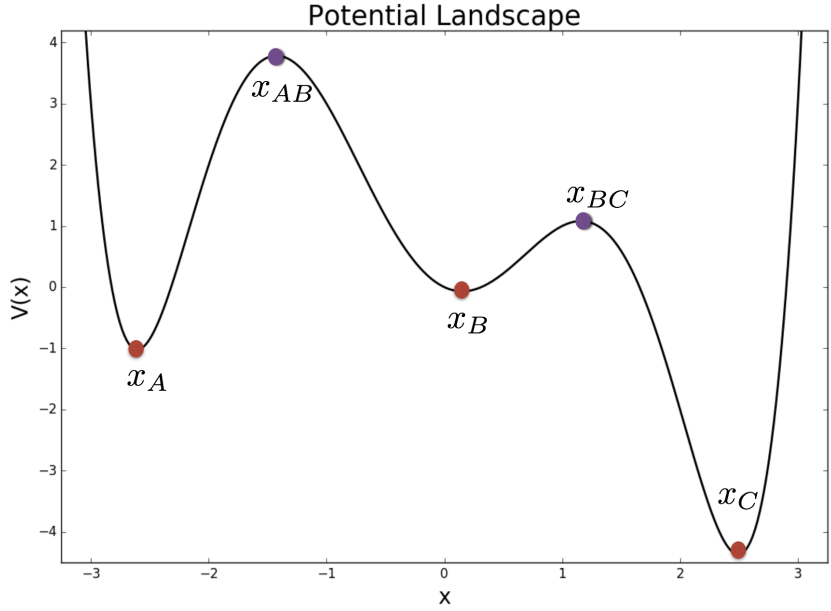


Figure 3: [Color online] The sixth-order polynomial potential function. There are three local minima and two local maxima which correspond to saddle points in phase space.

friction in the system. With a large amount of friction, the transition simply passes through the saddle  $x_{AB}$  and slides into  $x_B$  as a solution to 13; however with less friction 13 may no longer have a infinite time solution with boundary conditions  $x_{AB}$  and  $x_B$ . Physically, this corresponds to the situation where the particle starts at the saddle  $x_{AB}$  with infinitesimal velocity to the right, builds up enough momentum due to insufficient friction, so that after passing  $x_B$  it overcomes the small barrier given by  $x_{BC}$  and eventually settles at  $x_C$ . In this case there is no dynamical path from  $x_{AB} \rightarrow x_B$ , but there is a dynamical path from  $x_{AB} \rightarrow x_C$ . Note with even less friction it is still possible for the heteroclinic connection from  $x_{AB}$  to  $x_B$  to exist again (the particle can bounce back), but we focus on the case where this connection doesn't exist. Naturally, this phenomenon of potential-well-skipping will be pronounced if  $U(x_{BC}) - U(x_B) \ll U(x_{AB}) - U(x_B) \ll U(x_{BC}) - U(x_C)$ .

There are two reasonable possibilities for the global action minimizer, when the boundary conditions are  $x_A$  and  $x_B$  (equipped with zero velocity) and yet there is no heteroclinic connection from  $x_{AB}$  to  $x_B$ . The first corresponds to the dynamical paths / time-reversed paths  $x_A \rightarrow x_{AB} \rightarrow x_C \rightarrow x_{BC} \rightarrow x_B$ . In this case, the local minimal action value of the Freidlin-Wentzell action is

$$A_{\text{loc}} = 4(U(x_{AB}) - U(x_A) + U(x_{BC}) - U(x_C)) \quad (32)$$

The second possibility corresponds to  $x_A \rightarrow x_{AB} \rightarrow x_B$ , but the instanton from  $x_{AB}$  to  $x_B$  is no longer given by a simple deterministic dynamics. This possibility happens if it is more efficient to minimize the action by deviating away from the deterministic path and using

noise to slow down the particle so that it settles at  $x_B$ . Naturally, this is the case if the difference  $U(x_{BC}) - U(x_C)$  is sufficiently large, corresponding to a deep well at location  $x_C$ . Then, the first possibility is not optimal as the particle needs a lot of noise to crawl back into the well of  $x_B$ , and it would rather spend a small amount of noise to slow down in the well of  $x_B$  before getting trapped in the well of  $x_C$ .

To be more specific, parameters used for producing Figure 3 are

$$[a_1, a_2, a_3, a_4, a_5, a_6] = \frac{1}{120}[-108, 364, -15, -135, 3, 11],$$

so that

$$x_A = -2.607291444942787, x_{AB} = -1.4251363637044439, x_B = 0.152393839371333, \quad (33)$$

$$x_{BC} = 1.1586416396791057, \text{ and } x_C = 2.494119602324065 \quad (34)$$

and

$$\begin{aligned} U(x_{AB}) - U(x_A) &= 19.22792801, U(x_{AB}) - U(x_B) = 15.41318608, \\ U(x_{BC}) - U(x_B) &= 4.59671282, \text{ and } U(x_{BC}) - U(x_C) = 21.8046503 \end{aligned}$$

In this case, when  $\gamma = 1$  there exists a heteroclinic connection between  $x_{AB}$  and  $x_B$ , whereas when  $\gamma = 0.75$  there no longer exists a heteroclinic connection<sup>1</sup>. Figure 5 shows the basins of attraction for the  $\gamma = 0.75$  system, approximated by numerical simulations of a large amount of initial conditions. Zooming in close to  $x_{AB}$  one sees that the basin of attraction for  $x_C$  had been eroded away, cutting off any noiseless transition from  $x_{AB}$  to  $x_B$ .

The deterministic path, streamlines, and a minimizer of the Freidlin-Wentzell action (computed by the method in §3.3) for  $\gamma = 1$  and  $\gamma = 0.75$  are shown in Figure 4. One can see that the deterministic path corresponding to  $\gamma = 1$  (going downhill from the point  $x_{AB}$ ) settles to the point  $x_B$ , and the minimizer and the deterministic path coincide.

When  $\gamma = 0.75$ , however, the deterministic path ends up in the well corresponding to location  $x_C$  whereas the a local minimizer of the Freidlin-Wentzell action ends directly ends at  $x_B$ . The action value for the minimizing path is less than  $\sim 10^{-2}$ , meaning that the most likely transition from  $x_A$  to  $x_B$  does not go through  $x_C$ , since this would correspond to an addition of 21.8046503 to the action. The minimizer was found by solving the Euler-Lagrange equations, but with a sufficiently good initialization the string method can also converge to the same solution. Since a sufficiently good initialization of the string seemed hard to find in our numerical experiments and  $\gamma$ -dependent<sup>2</sup>, our opinion is that it is safer to solve the 4th-order boundary value problem if “skipping” occurs.

---

<sup>1</sup>The gamma for which this bifurcation first occurs appears is between 0.76 and 0.75.

<sup>2</sup>We found no single initial string configuration that worked for both  $\gamma = 0.75$  and  $\gamma = 0.25$  without transitioning to  $x_C$ .

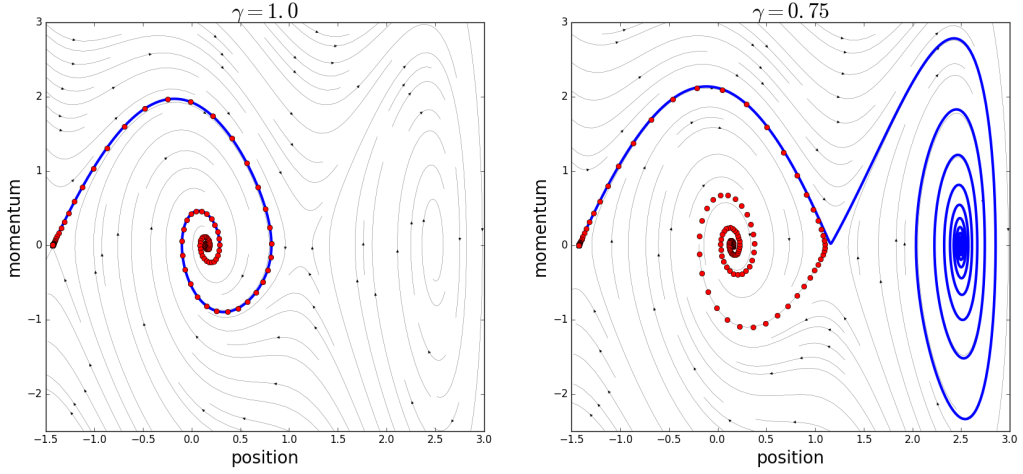


Figure 4: [Color online] Solution to the boundary value problem (red dots) and the dynamical trajectory (blue) for the Langevin system with a sixth order polynomial potential. The black lines are the stream lines corresponding to the phase portrait of the system. On the left we have a friction coefficient of  $\gamma = 1$ , and the dynamical trajectory corresponds to minimizers of the Freidlin-Wentzell action. On the right the friction coefficient is  $\gamma = 0.75$  and the dynamical trajectory no longer coincides with the action minimizer.

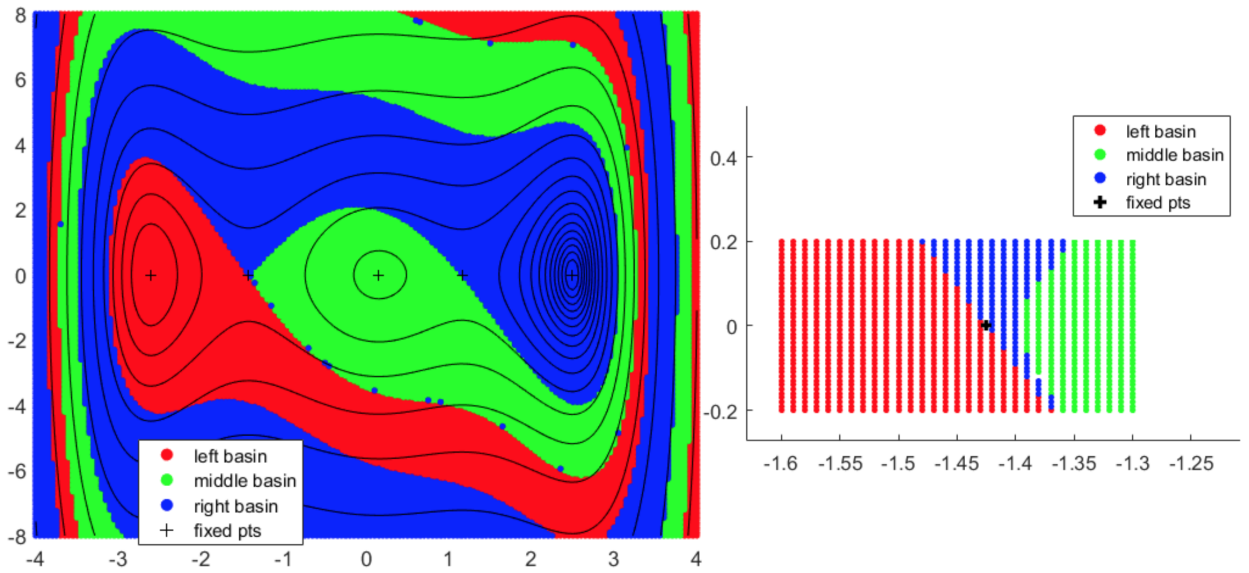


Figure 5: [Color online] Basins of attraction for the Langevin system with the sixth order polynomial potential and  $\gamma = 0.75$ .

*Recommendation.* The first recommendation is to compute the overdamped string and then simulate deterministic dynamics §3.2. If the trajectories of the Langevin system end up in the same potential minima as was computed in the overdamped limit, then a good local minimizer of the action is found. If the trajectories end up in a potential minimum different from  $x_A$  and  $x_B$ , then plan B is to apply the adapted string method §3.1. If that again results in an insertion of an unwanted minimum in the middle of the transition (e.g.,  $x_A \rightarrow x_{AB} \rightarrow x_C \rightarrow x_{BC} \rightarrow x_B$  discussed above), the String method may have skipped a better action minimizer too. The last recourse then is to attempt to directly minimize the Freidlin-Wentzell action (see §3.3). This, of course, presents additional difficulties since it may be computationally expensive (depending on the structure of the problem).

#### 4.3. Position dependent, matrix-valued friction coefficient

As the different effects of large and small scalar friction coefficients were described above, it is not difficult to see if the friction coefficient is a constant matrix with both small and large eigenvalues, then a mixed effect can be induced by this anisotropy, which further complicates the transition. Details of the case of a constant but anisotropic friction coefficient will no longer be individually discussed for conciseness; instead, in this section we show that the anisotropy only needs to be a local effect in order to result in a global change.

More precisely, consider an example with the potential

$$U(x, y) = \frac{1}{4} (x^2 - 1)^2 - \cos(\omega y)/\omega^2, \quad (35)$$

where  $\omega = 10$ . The friction coefficient matrix is

$$\Gamma(x, y) = \begin{bmatrix} 1 & 0 \\ 0 & 1 \end{bmatrix} + e^{-5(x^2+y^2)} \begin{bmatrix} c-1 & c-\delta \\ c-\delta & c-1 \end{bmatrix} \quad (36)$$

where  $c = 10$  and  $\delta = 0.1$ . The anisotropy is local with respect to the friction coefficient, but notably occurs at a saddle point of the system — there the matrix is

$$\Gamma(0, 0) = \begin{bmatrix} c & c-\delta \\ c-\delta & c \end{bmatrix} \quad (37)$$

whose eigenpairs are  $\lambda = 2c-\delta$ ,  $v_\lambda = [1 \ 1]^T$  and  $\lambda = \delta$ ,  $v_\lambda = [1 \ -1]^T$ . The former corresponds to an overdamped direction but the latter underdamped, however both only near the origin.

We consider the transition from  $x_A = (-1, 0)$  to  $x_B = (1, 0)$  (again with zero velocities). If the friction coefficient is isotropic (i.e., a constant scalar), the minimizing trajectories of both the overdamped and the Langevin system are simply straight lines from  $x_A$  to  $x_B$ . The anisotropic position-dependent case is different. Utilizing the string method both adapted for the Langevin equation and for the overdamped equation leads to the scenarios in Figure 6. The computed local action minimizer ends up going through additional potential minimum (e.g.,  $x = -1, y = 2\pi/\omega$ ) and saddle points.

Given that we cannot guarantee this local minimizer is the global one, it is possible that a transition path that is more “direct” exists for this system, but the simple heteroclinic

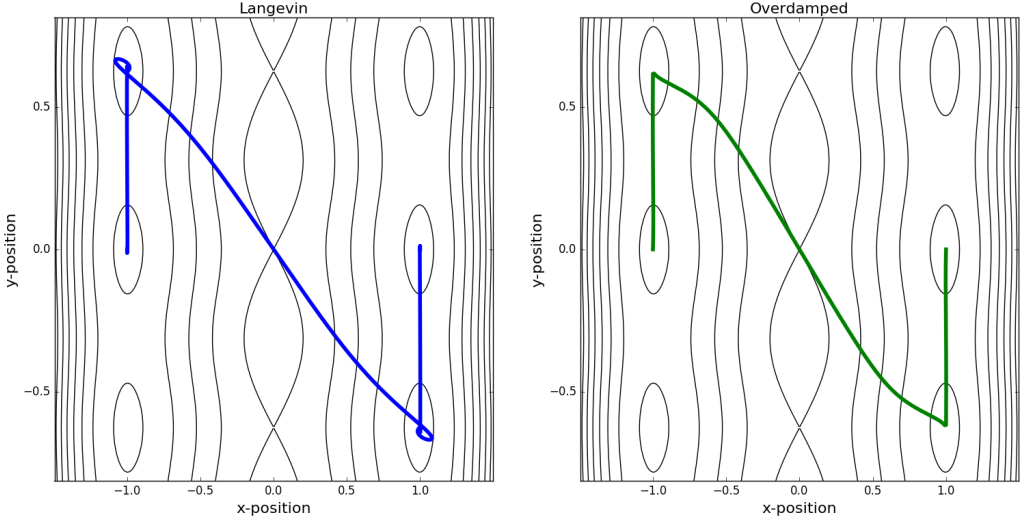


Figure 6: [Color online] The Langevin and overdamped instantons. Even though there is only a local change in the friction coefficient, the change in the instanton is global. The Langevin and overdamped instantons transition through similar saddles, but the oscillations usually present for the Langevin system are not well-represented due to limited resolution of the string calculation.

dynamics §3.2 do not exist. An approximation to the basin of attraction for the Langevin system is shown in Figure 7. There we see that there is no heteroclinic connection from  $(0, 0)$  to  $(1, 0)$  in the noiseless Langevin system. At least two points are clear: (i) The straight line transition path, present when friction is isotropic, is no longer optimal due to the new friction, and (ii) overdamped transition and Langevin transition projected to position space may not coincide when friction coefficient is not uniformly large everywhere.

*Recommendation.* To numerically compute the instanton, here we give the same recommendation as in §4.2; however, additional caution should be used about (i) utilizing the Euler-Lagrange equations, and (ii) computing transitions that involve more than two potential minima. Given the dependence of the friction coefficient on position, the Euler-Lagrange equations need to be modified from the constant coefficient case 22. Furthermore, if the transition involves more than two minima, the accuracy of the string method adapted to the Langevin equation may degrade as it tries to resolve multiple oscillatory regions. One can instead compute pairwise transitions between minima, and then concatenate.

*Two overdamped limits.* It is also important to clarify, in the position-dependent friction case, what is an overdamped limit of

$$\begin{aligned} dq &= pdt \\ dp &= -\nabla U(q)dt - \Gamma(q)pdt + \epsilon\Gamma(q)^{1/2}dW. \end{aligned} \tag{38}$$

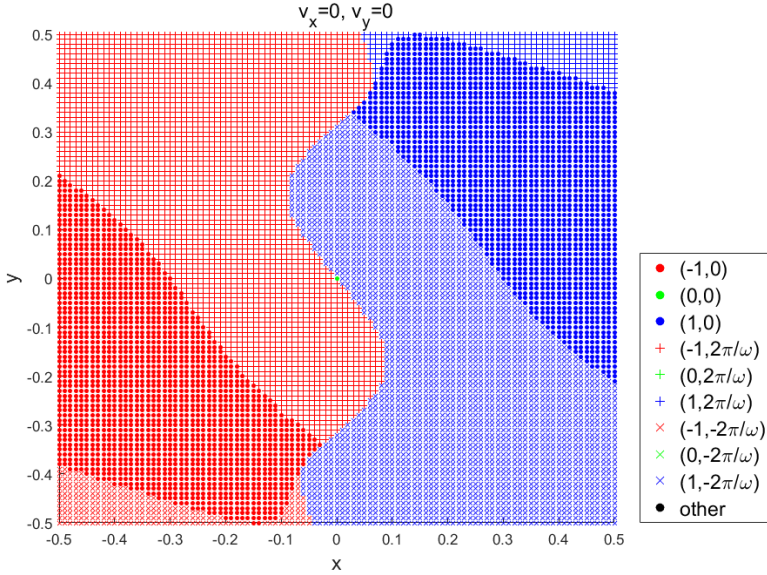


Figure 7: [Color online] The basins of attraction for the position dependent friction coefficient in the Langevin system, with a velocity perturbation direction  $\mathbf{v} = 0$ . We also considered various other velocity perturbation directions (not shown; available upon request) and were led to a similar structure as shown above.

The overdamped result in Figure 7 was computed from a formal limit,

$$dq = -\Gamma(q)^{-1} \nabla U(q) dt + \epsilon \Gamma(q)^{-1/2} dW. \quad (39)$$

Repeating the derivation in §2, it is not difficult to see that, under the condition of existences of needed heteroclinic orbits, the formal limit 40 provides minimum action values consistent with those of the full system 38. Because of this, we used this formal limit to investigate the rare event of metastable transition.

Note, however, that this formal limit does not conserve the  $q$  marginal of the Boltzmann-Gibbs distribution,  $Z^{-1} \exp(-(p^2/2 + U(q))/(\epsilon^2/2)) dq dp$ , which however remains as an invariant distribution of the Langevin equation 38 despite of the no-longer-constant friction coefficient. One can show, by solving the stationary Fokker-Planck equation, that the following corrected overdamped limit preserves the marginal Boltzmann-Gibbs,

$$dq = \left( -\Gamma(q)^{-1} \nabla U(q) + \frac{\epsilon^2}{2} \nabla A(q) \right) dt + \epsilon \Gamma(q)^{-1/2} dW, \quad (40)$$

where  $A(q) := \Gamma(q)^{-1}$ . This equation is in fact consistent with the variable friction small mass limit in the literature, and we refer to [10] for more discussions (including convergence of the dynamics, not just long term statistics) and references.

We chose not to further investigate rare events in this correction (40) though, because its large deviation structure is in fact unclear (one cannot simply remove the  $\nabla A$  term via  $\epsilon \rightarrow 0$ , since the noise also scales). An investigation could be interesting but it is out of the scope of this article, as our approach directly provided a solution to the full problem 38.

#### 4.4. Velocity dependent, matrix-valued friction coefficient

Although complications previously investigated in 4.2 and 4.3 can all add up to this case, to avoid redundancy we concentrate on the differences that a velocity dependence can induce. We do so by revisiting the Mueller potential with an anisotropic velocity dependent friction coefficient matrix in a mildly underdamped situation. When the friction coefficient depends on velocity, generally there is no analogous overdamped limit any more, and the system

$$\begin{aligned} dq &= pdt \\ dp &= -\nabla U(q)dt - \Gamma(q, p)pdt + \epsilon\Gamma(q, p)^{1/2}dW. \end{aligned} \quad (41)$$

may not even admit Boltzmann-Gibbs as an invariant distribution any more. In terms of nonequilibrium statistics, we show the velocity dependence modifies instantons.

More specifically, consider an example where  $\Gamma$  only depends on  $p = [\dot{x}, \dot{y}]$ , in the form of

$$\Gamma(\dot{x}, \dot{y}) = \begin{bmatrix} 5 + \exp(\dot{x}) + \exp(\dot{y}) & 1.25 \\ 1.25 & 5 + \exp(-\dot{x}) + \exp(-\dot{y}) \end{bmatrix} \quad (42)$$

Note  $\Gamma(\dot{x}, \dot{y}) \neq \Gamma(-\dot{x}, -\dot{y})$ ; thus we need to pay special attention to the time-reversed Langevin equation as well, see §2.

In Figure 8 we compute the same transition from §4.1, but with 42. Here there is a difference between time-reversed dynamics and regular Langevin dynamics since the friction coefficient matrix is not symmetric with respect to sign reversal of velocity. The true minimizing path, is a concatenation of the green curves or the blue curves depending on which transition one is interested. The string method or dynamics can still be utilized to compute the minimizing trajectory, but twice the computation is necessary.

The difference between time-reversed dynamics and regular dynamics can lead to significant complications. Given the phenomena in §4.2, heteroclinic connections that exist in

$$\ddot{\mathbf{x}} + \Gamma(\dot{\mathbf{x}})\dot{\mathbf{x}} + \nabla U = 0 \quad (43)$$

do not necessarily have an analog in

$$\ddot{\mathbf{x}} + \Gamma(-\dot{\mathbf{x}})\dot{\mathbf{x}} + \nabla U = 0. \quad (44)$$

*Recommendation.* Even though there is no analogous overdamped limit, one can still utilize knowledge of the string in the overdamped limit to compute instantons for this system. To make use of the overdamped limit, use the friction coefficient matrix  $\Gamma(\mathbf{x}, \dot{\mathbf{x}} = 0)$  and compute the overdamped string. This is, in a general setup, a position-dependent-friction string calculation as in §4.3. Then one can use the method of dynamics §3.2 to compute trajectories for the Langevin equation and time-reversed Langevin equation. If the resulting noiseless (modified) Langevin trajectories do not end up at the target minima, then one can also evolve two strings, one corresponding to Langevin dynamics and the other to the time-reversed dynamics, to compute a local action minimizer. If the previous methods fail and if it is feasible to do so, one can try to compute minimizers utilizing the Euler-Lagrange equations.

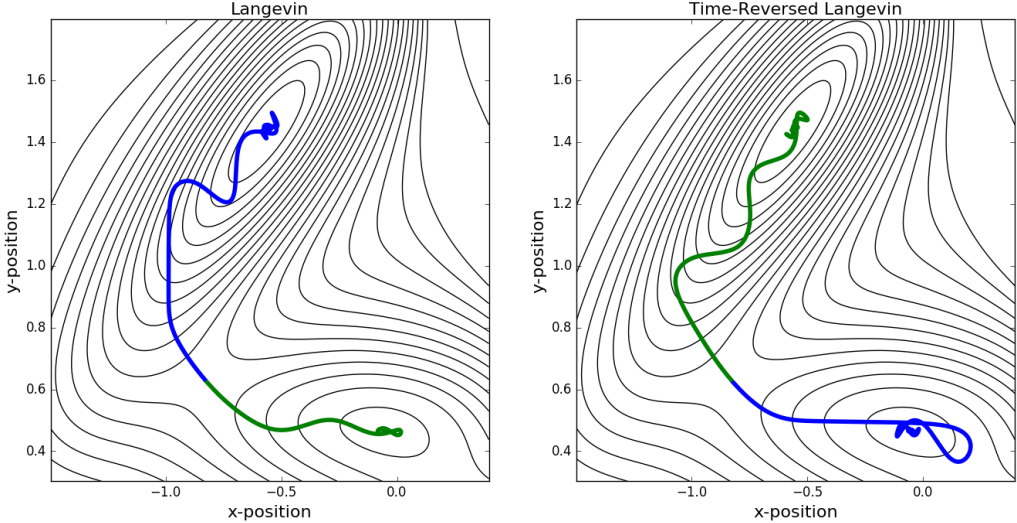


Figure 8: [Color online] Strings of the Langevin equation corresponding to a velocity dependent friction coefficient. For this case the strings are no longer instantons. The true instanton is a concatenation of the blue strings or a concatenation of the green strings depending on which fixed point is the start of the interested transition.

## 5. Conclusion

To illustrate what features one can see in inertial Langevin metastable transitions that differ from the familiar overdamped picture, we computed minimizers of the Freidlin-Wentzell action for the Langevin equation with respect to various types of friction coefficients. The computation was enabled as we showed the possibility of calculating a local minimizer of the Freidlin-Wentzell action, based on exploiting structures of the action function. These structures led to a simple modification of the string method and the introduction of an approach based on dynamics for quickly obtaining minimizing paths. We have shown that, depending on the amount of damping present in the system, both the transition rates and the transition paths can be different from those obtained by overdamped dynamics. Furthermore, we have shown that it is possible to calculate instantons for position and velocity-dependent friction coefficients. If the friction coefficient was asymmetric with respect to a sign change of velocity, the instanton needs to be computed utilizing two different equations.

## 6. Acknowledgment

MT is partially supported by NSF grant DMS-1521667. MT is grateful for valuable discussions with Tony Lelièvre and encouragements from Jianfeng Lu to continue exploring this interesting problem.

## Appendix A. Perturbation Direction

Suppose that  $\mathbf{v}$  is an eigenvector of the matrices  $A, B, C, D$  with eigenvalues  $\lambda_A, \lambda_B, \lambda_C, \lambda_D$  respectively. Then

$$\begin{bmatrix} \alpha\mathbf{v} \\ \beta\mathbf{v} \end{bmatrix} \quad (\text{A.1})$$

is an eigenvector of the matrix

$$\begin{bmatrix} A & B \\ C & D \end{bmatrix} \quad (\text{A.2})$$

with eigenvalues

$$\lambda = \frac{\lambda_A + \lambda_D \pm \sqrt{(\lambda_A - \lambda_D)^2 + 4\lambda_B\lambda_C}}{2} \quad (\text{A.3})$$

and

$$\frac{\beta}{\alpha} = \frac{\lambda_A - \lambda_D \pm \sqrt{(\lambda_A - \lambda_D)^2 + 4\lambda_B\lambda_C}}{2\lambda_B} \quad (\text{A.4})$$

with appropriate modifications for the  $\lambda_B = 0$  case. The derivation is as follows: Starting with the ansatz for the eigenvector we compute

$$\begin{bmatrix} A & B \\ C & D \end{bmatrix} \begin{bmatrix} \alpha\mathbf{v} \\ \beta\mathbf{v} \end{bmatrix} = \begin{bmatrix} (\lambda_A + \frac{\beta}{\alpha}\lambda_B)\mathbf{I} & 0 \\ 0 & (\lambda_C\frac{\alpha}{\beta} + \lambda_D)\mathbf{I} \end{bmatrix} \begin{bmatrix} \alpha\mathbf{v} \\ \beta\mathbf{v} \end{bmatrix} \quad (\text{A.5})$$

and we choose the parameters  $\alpha$  and  $\beta$  such that the diagonals of the matrix are equal.

With respect to the Langevin equation with a constant friction coefficient matrix  $\Gamma$ , and Hessian of the potential  $H$ , the Hessian of the Langevin system is the following block matrix

$$H_L = \begin{bmatrix} 0 & \mathbf{I} \\ -H & -\Gamma \end{bmatrix}. \quad (\text{A.6})$$

Assume that  $\Gamma$  and the  $H$  share an eigenvector  $\mathbf{v}$ , as for example would be the case for an isotropic friction coefficient. Based off of the previous calculations the eigenvector and values are

$$\mathbf{v}_L = \begin{bmatrix} \mathbf{v} \\ \beta\mathbf{v} \end{bmatrix} \quad (\text{A.7})$$

where

$$\alpha = 1 \quad (\text{A.8})$$

$$\beta = \frac{-\lambda_\Gamma + \sqrt{(\lambda_\Gamma)^2 - 4\lambda_H}}{2} \quad (\text{A.9})$$

$$(\text{A.10})$$

and  $\beta$  is an eigenvalue. Along an unstable direction  $\lambda_H < 0$  and in the limit  $\lambda_\Gamma \rightarrow \infty$  we have  $\beta = \frac{\sqrt{-\lambda_H}}{\lambda_\Gamma} + \mathcal{O}\left(\frac{\lambda_H}{(\lambda_\Gamma)^2}\right)$ .

We can estimate  $\lambda_H$  by taking a few time-steps along the perturbation direction of a well-resolved string since

$$\begin{aligned} x(t_0) &\approx x^* + be^{-\lambda_H t_0} \\ x(t_1) &\approx x^* + be^{-\lambda_H t_0 + \Delta t} \\ x(t_2) &\approx x^* + be^{-\lambda_H t_0 + 2\Delta t} \end{aligned}$$

where  $t_j = t_0 + \Delta t$  and  $x^*$  is a fixed point. Thus our estimate is

$$-\lambda_H \approx \frac{1}{\Delta t} \ln \left( \frac{x(t_2) - x(t_1)}{x(t_1) - x(t_0)} \right).$$

To utilize this any component of the vector works. Using the perturbed direction for momentum seems to have little effect on the cases considered here. That is to say one could just take the perturbation direction for velocity to be zero and in all cases that we have examined the resulting trajectory was similar.

## References

### References

- [1] M. Freidlin, A. Wentzell, Random Perturbations of Dynamical Systems, 3rd Edition, Springer, 2012.
- [2] A. Dembo, O. Zeitouni, Large Deviations Techniques and Applications, 2nd Edition, Springer, 2010.
- [3] W. E, W. Ren, E. Vanden-Eijnden, String method for the study of rare events, *Phys. Rev. B* 66 (2002) 052301. doi:10.1103/PhysRevB.66.052301.  
URL <https://link.aps.org/doi/10.1103/PhysRevB.66.052301>
- [4] W. E, W. Ren, E. Vanden-Eijnden, Simplified and improved string method for computing the minimum energy paths in barrier-crossing events, *The Journal of Chemical Physics* 126 (16) (2007) 164103. arXiv:<https://doi.org/10.1063/1.2720838>, doi:10.1063/1.2720838.  
URL <https://doi.org/10.1063/1.2720838>
- [5] U. Titulaer, A systematic solution procedure for the fokker-planck equation of a brownian particle in the high-friction case, *Physica A: Statistical Mechanics and its Applications* 91 (3) (1978) 321 – 344. doi:[https://doi.org/10.1016/0378-4371\(78\)90182-6](https://doi.org/10.1016/0378-4371(78)90182-6).  
URL <http://www.sciencedirect.com/science/article/pii/0378437178901826>
- [6] E. Nelson, Dynamical Theories of Brownian Motion, 2nd Edition, Princeton University Press, 2001.
- [7] C. W. Gardiner, Handbook of Stochastic Methods, 2nd Edition, Springer, 1985.
- [8] G. A. Pavliotis, Stochastic Processes and Applications: Diffusion Processes, the Fokker-Planck and Langevin Equations, 1st Edition, Springer-Verlag New York, 2014.
- [9] K. A. Newhall, E. Vanden-Eijnden, Averaged equation for energy diffusion on a graph reveals bifurcation diagram and thermally assisted reversal times in spin-torque driven nanomagnets, *Journal of Applied Physics* 113 (18) (2013) 184105. arXiv:<https://doi.org/10.1063/1.4804070>, doi:10.1063/1.4804070.  
URL <https://doi.org/10.1063/1.4804070>

[10] S. Hottovy, A. McDaniel, G. Volpe, J. Wehr, The smoluchowski-kramers limit of stochastic differential equations with arbitrary state-dependent friction, *Communications in Mathematical Physics* 336 (3) (2015) 1259–1283.

[11] H. L. Tepper, G. A. Voth, Mechanisms of passive ion permeation through lipid bilayers: Insights from simulations, *J Phys Chem B* 110 (42) (2006) 21327–21337. doi:10.1021/jp064192h.

[12] M. Urbakh, J. Klafter, D. Gourdon, J. Israelachvili, The nonlinear nature of friction, *Nature* 430 (2004) 525 EP –.

URL <http://dx.doi.org/10.1038/nature02750>

[13] H. Olsson, K. strm, C. C. de Wit, M. Gfvert, P. Lischinsky, Friction models and friction compensation, *European Journal of Control* 4 (3) (1998) 176 – 195. doi:[https://doi.org/10.1016/S0947-3580\(98\)70113-X](https://doi.org/10.1016/S0947-3580(98)70113-X)

URL <http://www.sciencedirect.com/science/article/pii/S094735809870113X>

[14] H. Levine, W.-J. Rappel, I. Cohen, Self-organization in systems of self-propelled particles, *Physical Review E* 63 (1) (2000) 017101.

[15] M. R. D'Orsogna, Y.-L. Chuang, A. L. Bertozzi, L. S. Chayes, Self-propelled particles with soft-core interactions: patterns, stability, and collapse, *Physical review letters* 96 (10) (2006) 104302.

[16] P. P. Eggleton, L. G. Kiseleva, P. Hut, The equilibrium tide model for tidal friction, *The Astrophysical Journal* 499 (2) (1998) 853.

[17] R. A. Mardling, D. Lin, Calculating the tidal, spin, and dynamical evolution of extrasolar planetary systems, *The Astrophysical Journal* 573 (2) (2002) 829.

[18] T. Grafke, T. Schäfer, E. Vanden-Eijnden, *Long Term Effects of Small Random Perturbations on Dynamical Systems: Theoretical and Computational Tools*, Springer New York, New York, NY, 2017, pp. 17–55. doi:10.1007/978-1-4939-6969-2\_2.

URL [https://doi.org/10.1007/978-1-4939-6969-2\\_2](https://doi.org/10.1007/978-1-4939-6969-2_2)

[19] E. Forgoston, R. O. Moore, A primer on noise-induced transitions in applied dynamical systems, *SIAM Review* (2017) accepted.

[20] F. Bouchet, J. Reygner, Generalisation of the eyring–kramers transition rate formula to irreversible diffusion processes, *Annales Henri Poincaré* 17 (12) (2016) 3499–3532. doi:10.1007/s00023-016-0507-4.

URL <https://doi.org/10.1007/s00023-016-0507-4>

[21] M. Tao, Hyperbolic periodic orbits in nongradient systems and small-noise-induced metastable transitions, *Physica D* 363 (15) (2018) 1–17.

[22] W. E, W. Ren, E. Vanden-Eijnden, Minimum action method for the study of rare events, *Communications on Pure and Applied Mathematics* 57 (5) (2004) 637–656. doi:10.1002/cpa.20005.

URL <http://dx.doi.org/10.1002/cpa.20005>

[23] X. Zhou, W. Ren, W. E, Adaptive minimum action method for the study of rare events, *The Journal of Chemical Physics* 128 (10) (2008) 104111. arXiv:<https://doi.org/10.1063/1.2830717>, doi:10.1063/1.2830717.

URL <https://doi.org/10.1063/1.2830717>

[24] X. Wan, An adaptive high-order minimum action method, *Journal of Computational Physics* 230 (24) (2011) 8669 – 8682. doi:<https://doi.org/10.1016/j.jcp.2011.08.006>.

URL <http://www.sciencedirect.com/science/article/pii/S0021999111004785>

[25] M. Heymann, E. Vanden-Eijnden, The geometric minimum action method: A least action principle on the space of curves, *Communications on Pure and Applied Mathematics* 61 (8) (2008) 1052–1117. doi:10.1002/cpa.20238.

URL <http://dx.doi.org/10.1002/cpa.20238>

[26] E. Vanden-Eijnden, M. Heymann, The geometric minimum action method for computing minimum energy paths, *The Journal of Chemical Physics* 128 (2008) 061103.

[27] M. Heymann, E. Vanden-Eijnden, Pathways of maximum likelihood for rare events in nonequilibrium systems: application to nucleation in the presence of shear, *Physical Review Letters* 100 (14) (2008) 140601.

[28] B. S. Lindley, I. B. Schwartz, An iterative action minimizing method for computing optimal paths in

stochastic dynamical systems, *Physica D: Nonlinear Phenomena* 255 (2013) 22–30.

[29] T. Grafke, R. Grauer, T. Schfer, The instanton method and its numerical implementation in fluid mechanics, *Journal of Physics A: Mathematical and Theoretical* 48 (33) (2015) 333001.  
 URL <http://stacks.iop.org/1751-8121/48/i=33/a=333001>

[30] L. C. G. Rogers, D. Williams, *Diffusions, Markov processes and martingales: Volume 2, Itô calculus*, Vol. 2, Cambridge university press, 1994.

[31] D. Nualart, *The Malliavin calculus and related topics*, Vol. 1995, Springer, 2006.

[32] C. Villani, *Hypocoercivity*, no. 949-951, American Mathematical Soc., 2009.

[33] L. Maragliano, A. Fischer, E. Vanden-Eijnden, G. Ciccotti, String method in collective variables: Minimum free energy paths and isocommittor surfaces, *The Journal of Chemical Physics* 125 (2) (2006) 024106. [arXiv:https://doi.org/10.1063/1.2212942](https://doi.org/10.1063/1.2212942), doi:10.1063/1.2212942.  
 URL <https://doi.org/10.1063/1.2212942>

[34] W. E, X. Zhou, The gentlest ascent dynamics, *Nonlinearity* 24 (6) (2011) 1831.  
 URL <http://stacks.iop.org/0951-7715/24/i=6/a=008>

[35] W. Ren, E. Vanden-Eijnden, A climbing string method for saddle point search, *The Journal of chemical physics* 138 (2013) 134105.

[36] D. Viswanath, Spectral integration of linear boundary value problems, *Journal of Computational and Applied Mathematics* 290 (2015) 159 – 173. doi:<http://dx.doi.org/10.1016/j.cam.2015.04.043>.  
 URL <http://www.sciencedirect.com/science/article/pii/S0377042715002691>

[37] J. Boyd, *Chebyshev and Fourier Spectral Methods*, 2nd Edition, Dover, 2001.

[38] D. P. Herzog, S. Hottovy, G. Volpe, The small-mass limit for langevin dynamics with unbounded coefficients and positive friction, *J Stat Phys* 163 (2016) 659–673. doi:<https://doi.org/10.1007/s10955-016-1498-8>.

[39] M. Freidlin, W. Hu, Smoluchowski-kramers approximation in the case of variable friction 179.

[40] M. Freidlin, W. Hu, A. Wentzell, Small mass asymptotic for the motion with vanishing friction, *Stochastic Processes and their Applications* 123 (1) (2013) 45 – 75. doi:<https://doi.org/10.1016/j.spa.2012.08.013>.  
 URL <http://www.sciencedirect.com/science/article/pii/S0304414912001901>